

# Evaluation of the Impact of Morphing Horizontal Tail Design of the UAS-S45 Performances

Marine Segui<sup>1</sup>, Ruxanda Mihaela Botez<sup>2</sup>, Éloïse Paper<sup>3</sup>  
and Jean-Charles Di-Mambro<sup>4</sup>

*ETS, Laboratory of Active Controls, Avionics and AeroServoElasticity LARCASE  
1100 Notre Dame West, Montreal, Quebec, Canada, H3C-1K3*

**N**owadays, increasingly sensitive to the global warming, the aerospace industry is committed to reduce its toxic gas emissions. To take a part in this global effort, a morphing study on the horizontal tail of an Unmanned Aerial System (UAS) is here presented. This type of morphing consists in changing the shape of the horizontal tail wing during the flight in order to improve aircraft aerodynamical characteristics. The geometry of the horizontal tail was changed as function of 3 parameters: the dihedral (from -80 degrees to +80 degrees), the sweep (from -80 degrees to +80 degrees) or the twist angles (from -50 degrees to 50 degrees). To measure the impact of these types of changes on the horizontal tail, an aerodynamic study was performed using the Vortex-Lattice Method (VLM) implemented in OpenVSP software (distributed by NASA). The methodology consists, in the first place, to develop a reference model that can reproduce the aerodynamic behavior of the reference aircraft with its horizontal tail. Then, morphing models were developed based on the reference model, in which different dihedral, sweep or twist angles were changed for its horizontal tail. Finally, a model able to trim the UAS-S45 for static cruise conditions was used to compute the thrust force required to balance the aircraft for each case (original and morphing). A gain of 6% of thrust has been obtained when the aircraft was trimmed using twist angle instead of elevators deflection.

## Introduction

In the context of global warming, the research and innovation activities are particularly offered to find solutions to make our future inventions more ecological. The aerospace sector is also impacted by this ecological aspect. In this way, the International Civil Aviation Organization (ICAO) has planned to reduce by 50% of the Carbon Dioxide (CO<sub>2</sub>) emissions registered in 2005 before 2050 [1]. To reach this major objective, it is necessary to find solutions that can render the future aircraft greener than it is today. Several studies on optimization of airlines trajectories have shown that around 3% of fuel could be saved for a single travel [2-10]. Another idea consists in optimizing engines systems, in this way; simulations have shown that it is possible to develop accurate models of engines behavior. These generating data could then be used in a performance model, able to predict the fuel that is going to be consumed and thus saved for a given flight [11-13].

---

<sup>1</sup> PhD. Student, LARCASE, 1100 Notre Dame West, Montréal, QC, H3C-1K3, Canada

<sup>2</sup> Full Professor, Canada Research Chair Holder Level 1 in Aircraft Modeling and Simulation Technologies, ETS, LARCASE, 1100 Notre Dame West, Montréal, QC, H3C-1K3, Canada

<sup>3</sup> Undergraduate Student, LARCASE, 1100 Notre Dame West, Montréal, QC, H3C-1K3, Canada

<sup>4</sup> Undergraduate Student, LARCASE, 1100 Notre Dame West, Montréal, QC, H3C-1K3, Canada

In addition to these two promising studies, there is also a third methodology that could be used to improve the aerospace sector emissions. This methodology is based on a geometrical modification of the wing along the flight in order to adapt its aerodynamic performances required during the flight. This technique is called « Morphing-Wing » and can be applied on using different techniques such as the distortion of the airfoil or the winglet along the flight [14-24].

As part of a morphing study, the LARCASE team has conducted a morphing study on the business jet Cessna Citation X. For this study, the horizontal tail was modified (morphed) in order to balance the aircraft without using a stabilizer angle while minimizing the thrust required during cruise. This study has shown up to 4 % of fuel saved on average, that is considered a very good performance [25]-[26]. It is important to precise that the Cessna Citation X is an aircraft that flies at Mach number 0.85 in cruise, which corresponds to the transonic regime, and consequently, it is enough difficult to well predict its aerodynamic characteristics. This study was lead to demonstrate that if the morphing wing shows efficient results in a low subsonic domain, then, it could partially validate the performance observed in the Cessna Citation X aircraft study. The word “partially” is used because it is most accurate to compute results using Navier-Stocks methods than Vortex Lattice method (VLM) methods for a validation study, but the behavior in the subsonic regime is still very well predicted with simplified methods such as VLM, thus results that will be obtained using VLM could be considered as faithful [27].

The research performed on the horizontal tail of the UAS-S45 is presented in three main sections. The first section is dedicated to present the methodology used to model the original behavior of the UAS-S45 at an aerodynamic and a performance level. Then, based on reference models (i.e. corresponding to the original configuration of the UAS) designed, the second section presents the way in which the morphing-wing techniques are applied on the aircraft and their way of measuring. The final third section is dedicated to the presentation of results obtained for this study, thereby, the thrust required by the original UAS configuration is compared with and the morphed-one to be operated at different flight conditions.

### **I – Design of UAS-S45 reference models**

This first section is dedicated to present how the UAS-S45 is modeled to perform this research. Indeed, to be able to measure the impact of the horizontal tail morphing application on the UAS-S45, it is first necessary to design a model of its original configuration.

The UAS-S45 is a military unmanned aerial system designed by the Mexican company Hydra, and is conventionally used for oversight missions (see Fig. 1). Table 1 shows some general characteristics of the UAS-S45 in terms of dimensions, areas, performances and motorization.

To design its aerodynamic model based on its geometrical characteristics, several methods and software are available but their choice was done according to the flight domain of the UAS (under Mach number of 0.3) and from an optimization point of view where the computation time needed to be quick enough. From these criteria, OpenVSP was the software chosen to perform the aerodynamic study [28]-[29]. Designed by the NASA, and available to the

public since 2002, OpenVSP is an open-source software that allows to design an aircraft, and to further compute its aerodynamic characteristics (i.e. lift, moments, induced and parasite drag, etc.).

Vortex-Lattice (VLM) and Panel methods are the two aerodynamic resolution methods available in the OpenVSP package. These two methods are particularly efficient when they are to model basic wing shapes in a low subsonic flow (meanwhile, it has been shown that OpenVSP software was accurate aircraft modeling for aerodynamic up to Mach number of 0.6 and for angles of attack lower than 5 degrees [30]), which corresponds exactly to the flight range of the UAS.

**Table 1. UAS-S45 characteristics**

<b>Designation</b>	<b>Value</b>
<u>Dimensions</u>	
Wing span	6.11 m
MAC	0.57 m
Length	3.01 m
<u>Surface</u>	
Wing area	2.72 m <sup>2</sup>
<u>Performance</u>	
Maximum speed	90 kts
Cruise speed	50-55 kts
Maximum take-off weight	79.6 kg
Empty weight	57 kg
Service ceiling	20,000 ft
Operational range	120 km
<u>Engines</u>	
Number of engines	2
Configuration	Push-Pull



**Figure 1. UAS-S45<sup>5</sup>**

1) Aerodynamic Model of the UAS-S45 using OpenVSP software

To study the horizontal tail of the UAS-S45, it is necessary to model also the main wing in addition to the horizontal tail. Indeed, due to the flow downwash induced by the wing  $\varepsilon$ , the horizontal tail has a different angle of attack of the wing ( $\alpha_{WG} \neq \alpha_{HT}$ ). Because of the difficulty in prediction of the downwash  $\varepsilon$  the wing and the horizontal tail of the UAS-S45 were designed using the same model, in a way that the downwash was directly taken into account in the OpenVSP model. The fuselage and the vertical tails were not be modeled because it was considered that they were not influencing the aerodynamic coefficients calculated using the VLM computational method.

To design an aircraft, OpenVSP allows to use basic shapes pre-designed of a wing, a fuselage, etc. To modelize the wing and the horizontal tail of the UAS, two wing basic components were used. The main wing was designed using three wing-sections set using Table 2 data, and the horizontal tail was designed using two wing-sections that were set using Table 3 data. It is important to mention that the UAS-S45 has two vertical tails located under the horizontal

<sup>5</sup> CopyRight: <https://www.unmannedsystemstechnology.com/wp-content/uploads/2018/04/Hydra-Technologies-S45-Balaam-UAV.jpg>

tail, as a consequence, only the tip part of the horizontal tail would be morphed (i.e. the root part needs to be fixed due to vertical tails), this is the reason for which two sections were used to model the horizontal tail (see Fig. 2).

**Table 2. OpenVSP parameters to design the UAS-S45 wing**

<u>Designation</u>	<u>Value</u>
<u>Section 1 (wing)</u>	
Span	9.26 ft
Root Chord	2.20 ft
Tip Chord	1.29 ft
Sweep Angle	4.8 deg
Dihedral Angle	0.1 deg
Twist Angle	0.0 deg
Airfoil	NACA23015
<u>Section 2 (winglet part 1)</u>	
Span	0.40 ft
Root Chord	1.29 ft
Tip Chord	1.10 ft
Sweep Angle	20.0 deg
Dihedral Angle	5.0 deg
Twist Angle	0.0 deg
Airfoil	NACA0010
<u>Section 3 (winglet part 2)</u>	
Span	0.30 ft
Root Chord	1.10 ft
Tip Chord	0.40 ft
Sweep Angle	70.0 deg
Dihedral Angle	40.0 deg
Twist Angle	0.0 deg
Airfoil	NACA0010

**Table 3. OpenVSP parameters to design the UAS-S45 Horizontal Tail**

<u>Designation</u>	<u>Value</u>
<u>Section 1 (root part)</u>	
Span	0.85 ft
Root Chord	1.08 ft
Tip Chord	1.06 ft
Sweep Angle	8.1 deg
Dihedral Angle	0.0 deg
Twist Angle	0.0 deg
Airfoil	NACA0010
<u>Section 2 (tip part)</u>	
Span	1.39 ft
Root Chord	1.08 ft
Tip Chord	0.76 ft
Sweep Angle	8.1 deg
Dihedral Angle	0.0 deg
Twist Angle	0.0 deg
Airfoil	NACA0010

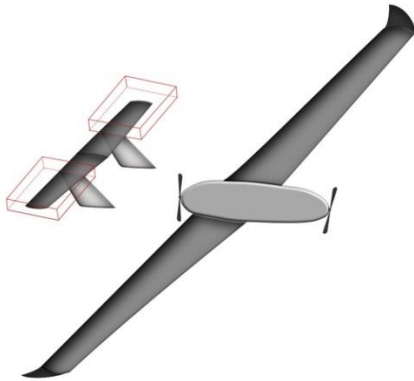
In addition, to complete the model, it was necessary to modelize elevators located at the trailing edge of the horizontal tail. OpenVSP allows to design control surfaces and for this reason, there is a menu dedicated to control surface dimensions and positions. Elevators were set to move from -20 to +15 degrees (where the positive sign signify downward motion and controversially, the negative sign signifies upward motion).

Figure 3 shows the aerodynamic model of the UAS-S45 that was designed using OpenVSP. Aerodynamic coefficients ( $C_L$ ,  $C_{D_i}$ , and  $C_m$ ) of the UAS-S45 were computed for angles of attack from -2 to 10 degrees, for Mach numbers from 0.10 to 0.18, and for elevators positions from -20 to +15 degrees using the VLM computational method.

It is important to precise that the VLM implemented in OpenVSP is able to give to the user, the lift coefficient  $C_L$ , all the drag coefficient  $C_{D_{tot}}$ ,  $C_{D_i}$  and  $C_{D_0}$  (Eq. 1), and the pitching moment coefficient  $C_m$ , that are useful for this study. The parasite drag  $C_{D_0}$  obtained using the VLM is the same for all configurations computed and under

estimated ( $C_{D_0} = 0.00507$ ). Consequently, to be able to well estimate the total drag, the parasite drag  $C_{D_0}$  was computed using Blasius skin friction law (for laminar flow conditions) [31] and added, as shown in Eq. (1), to the induced drag  $C_{D_i}$  already computed in order to obtain a total drag. As shown in Table 4,  $C_{D_0}$  was computed at 50 m/s, and for altitude of 5,000 ft and 20,000 ft.

$$C_{D_{tot}} = C_{D_i} + C_{D_0} \quad (1)$$



**Figure 2. Representation of the horizontal tails part that is going to be morphed**

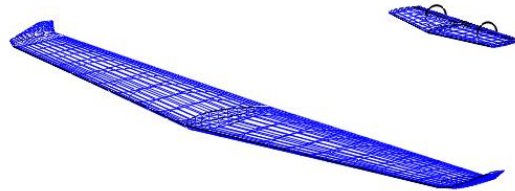


**Figure 3. Aerodynamic model of the UAS-S45 using OpenVSP software**

**Table 4. Parasite drag  $C_{D_0}$  computation**

Altitude	$S_{wet}$ Wing	$S_{wet}$ Horizontal tail	Form Factor (Hoerner)	$C_{D_0}$
5,000 ft	69.35 ft <sup>2</sup>	8.44 ft <sup>2</sup>	1.39	0.01082
20,000 ft			1.21	0.01170

In order to perform following steps of the study, all the aerodynamic coefficients computed ( $C_L$ ,  $C_{D_{tot}}$ , and  $C_m$ ) were finally be stocked in a table according to the Mach number, the angle of attack and the elevator deflection angle, as seen on Fig. 4.

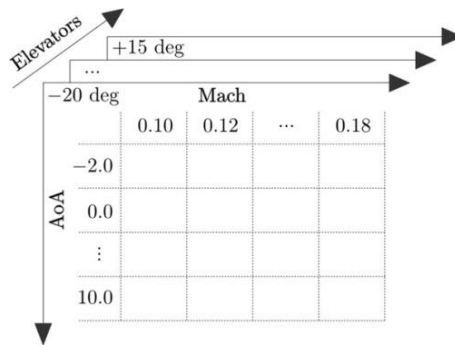


**Figure 4. Reference aerodynamic lookup table**

## 2) Design of the trim model for static cruise conditions

In order to evaluate the efficiency of the horizontal tail morphing, a model able to balance the UAS-S45 according to its configuration was designed. As said previously, aerodynamic coefficients are computed globally for the wing and the horizontal tail, without separating their contributions. Consequently, the trim model was designed by considering the wing and the horizontal tail as being in the same aerodynamic bloc. Fig. 5 shows forces and moments applied on the UAS-S45 while is performing a cruise.  $L$  and  $D$  are the aerodynamic forces (i.e. the Lift and the Drag),  $M_a$  is the aerodynamic moment generated at the Aerodynamic Center "AC",  $T$  is the engines thrust,  $P$  is the gravity force applied downward,  $M_e$  is the engine moment (applied at the engine center), and finally  $M_w$  is the moment due to the Weight applied at the Center of Gravity CG.

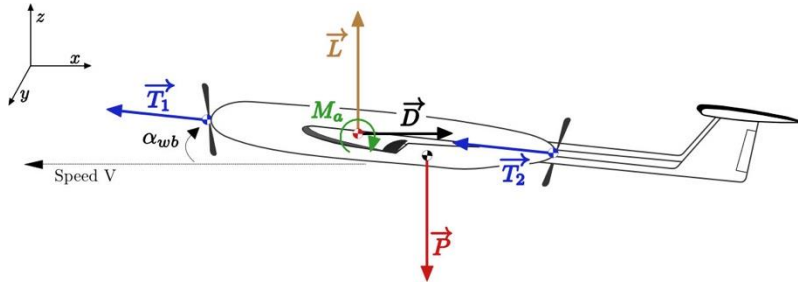


**Figure 5. Forces and moments considered to be applied on the UAS-S45 during cruise**

To balance the UAS-S45 during a cruise, the trim model (Fig. 6) will find the thrust required to solve the second Newton law as precised in Eqs. (2) for the given flight condition expressed in terms of precised inputs (i.e. an altitude, a gross weight, a centering and a Mach number), as follows.

$$\begin{aligned}
 \backslash x: \sum \vec{F}_x &= \vec{0} \Rightarrow D - T_{x1} - T_{x2} = 0 \\
 \backslash y: \sum \vec{M}_y &= \vec{0} \Rightarrow M_e + M_a + M_w = 0 \\
 \backslash z: \sum \vec{F}_z &= \vec{0} \Rightarrow L - P + T_{z1} + T_{z2} = 0
 \end{aligned} \tag{2}$$

It is important to precise that the center of application of the thrust generated from each engine is aligned to the gravity center according to the  $x$  axis, and consequently, the thrust has no lever arm. For this reason, the moment generates by engines was neglected.

To balance Eqs. (2) for a given flight condition, the trim model schematized in Fig. 6 was developed. As input, it required the flight condition, and as outputs, the angle of attack of the aircraft, the thrust required to balance the aircraft and the elevator position needed to perform stabilization were obtained. The «trim algorithm» is in charge of managing information that provided by inputs and by aerodynamic look-up tables (Fig. 4) in order to be able to compute the corresponding thrust.

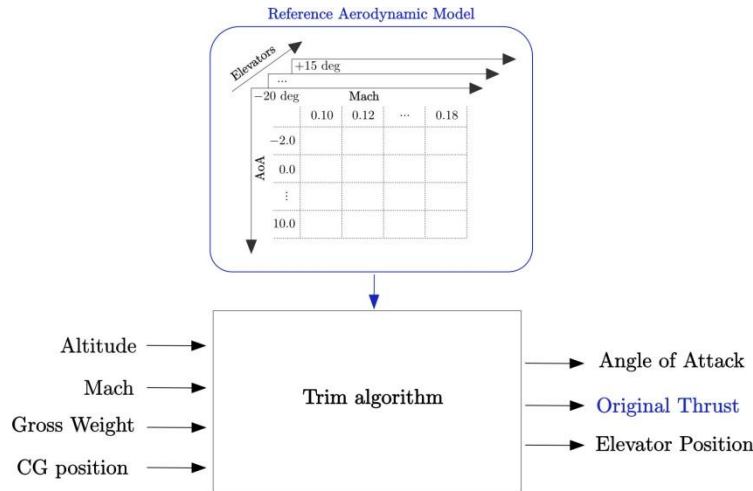


**Figure 6. Trim model for the reference UAS-S45 configuration**

The first step of the trim algorithm consists in finding the lift required to balance the gross weight of the aircraft, supposed as neutral initial thrust. Then, the lift required can be obtained by searching in the aerodynamic lookup-table given in Fig. 4, the angle of attack  $\alpha_{WG}$  that allows to obtain the corresponding “target-lift”. At this step, because of the fact that the angle of attack is known, the corresponding drag could also be evaluated from the lookup table (Fig. 4). Similarly, the elevator position required to balance the equation of moments can finally be found at the given angle of attack found before. This process was repeated until the difference in the angle of attack, the thrust, and the elevator position found between two consecutive iterations were found to be below a certain tolerance. Each iteration was initialized using an angle  $\alpha_{WG}$ , a thrust  $T$ , and an elevator deflection as the ones found in the previous iterations.

Several flight conditions will be considered for which the altitude changed from 5,000 ft to 20,000 ft, the gross weight from 75 kg to 65 kg and the Mach number from 0.10 to 0.16.

## II – Optimization of UAS-S45 cruise performances

In the previous sections it was shown how the original (non-morphed) UAS-S45 was modeled. In this section, the morphing that is supposed to be applied at the horizontal tail level of the UAS-S45 will be presented. Consequently, this section is divided in two sub-sections, the first sub-section presents the way in which the geometric deformations have been applied, and the second sub-section is dedicated to the presentation of the trim model for the morphing studies.

### 1) Geometrical Optimization

As presented above in Fig. 2 only tip sections of the horizontal tail could be modified because of the vertical tails locations. The morphing imagined in this way considered that this part of the horizontal tail could move according to a one degree of freedom along the flight. Three different types of motions were seen: one motion relative to the

dihedral angle, another motion relative to the sweep angle, and finally, the last one was done relative to the twist angle. The Fig. 7 gives an overview of morphing that will be studied.

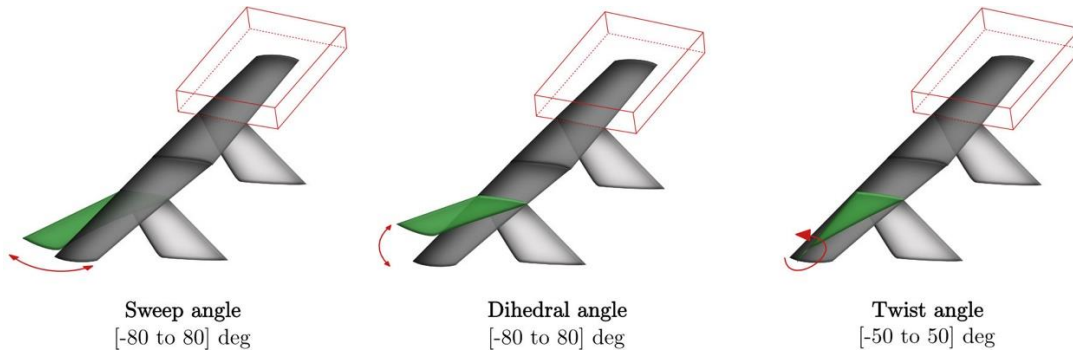


**Figure 7. Representation of the different morphing types tested**

Using the reference model, these morphing aircrafts have been modeled angles by changing the second wing section of the horizontal tail (Table 3) depending on the morphing angle selected (i.e. sweep, dihedral or twist). In the sweep angle morphing, the sweep angle was changed from -80 to 80 degrees, while other parameters were kept as constant in Table 3. Similarly, for the dihedral angle morphing, the dihedral angle was changed from -80 to 80 degrees, and for the twist morphing, the twist angle was changed from -50 to 50 degrees.

Finally, once they were parameterized, these configurations were given to the VLM solver of OpenVSP in order to compute their aerodynamic coefficients ( $C_L$ ,  $C_{D_i}$ , and  $C_m$ ) of the morphed UAS-S45 while depending on the morphing case, the morphed angle was varied. The total drag was computed as presented in the previous section. Aerodynamic data were stocked into lookup tables that could look as the tables shown in Fig. 8. It is important to note that, for morphing cases of twist, dihedral or sweep angles, the elevators deflection angles have been fixed to 0 degrees.

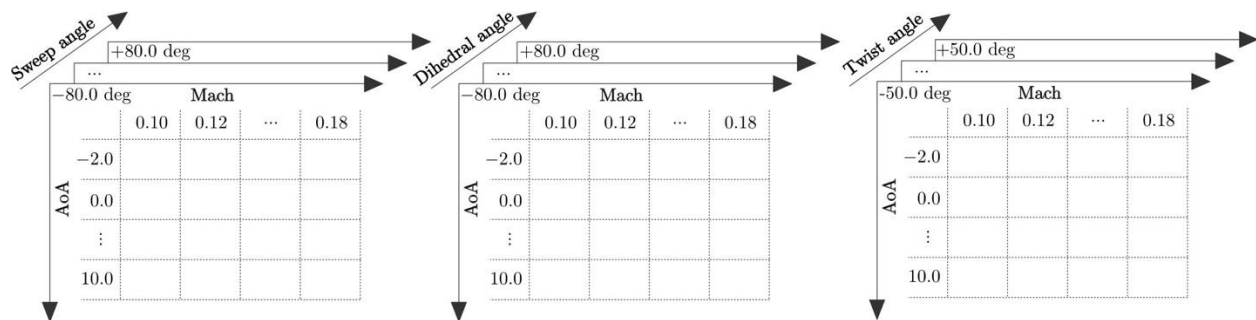


**Figure 8. Aerodynamic lookup tables for morphing configurations**



2) Trim of the UAS-S45 equipped with morphed horizontal tail for static cruise conditions

A similar model to the trim model dedicated to compute the reference state of the UAS-S45 (Fig. 6) is used to trim the morphed UAS-S45. Only a modification was made to balance the equation of moments. Indeed, instead of balancing the aircraft with an elevator deflection angle, the aircraft is balancing according to its morphing angle configuration (i.e. sweep, dihedral or twist). To sum up, in case of a morphing aircraft, the trim model gave as outputs: an angle of attack, a thrust force and a morphing angle (sweep, twist or dihedral depending on the case) (see Fig. 9).

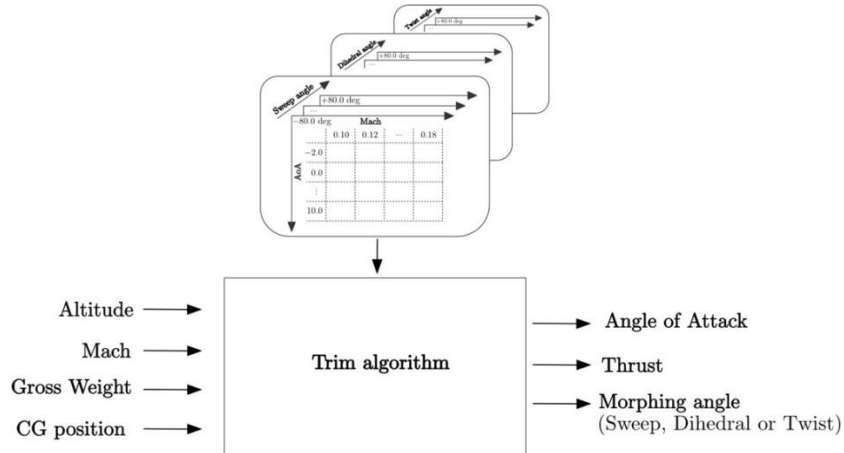


**Figure 9. Trim model used for the morphing configurations**

### III - Results

To show the efficiency of the performed morphing, a comparison was made between the thrust required to trim the UAS-S45 using the original configuration (with elevators in Section I), and the thrust required to trim a morphed aircraft equipped with an horizontal tail that would be able to move according to its dihedral angle, twist angle or its sweep angle (as seen in Section II). The Figure 10 shows the 12 flight conditions that were considerate in the study where the gross weight varies from 65 to 75 kg and the altitude from 5,000 ft to 20,000 ft. The Mach number was fixed for all flight conditions at 0.14, and the CG position was set to 25% of the Mean Aerodynamic Chord (MAC).

Figure 11 shows the Thrust (in Newton) computed in each reference or morphing cases for flight conditions selected. The darkest color is used to represent the reference case (i.e. where the UAS-S45 is trimmed using elevators). Moreover, this figure shows the relative gain of thrust obtained between the UAS-45 trimmed by elevators and another one trimmed using twist morphing. Generally, more thrust is required at low altitude (around 45 N at 5,000 ft) than at high altitude (around 32 N at 20,000 ft). More precisely, the thrust required for each morphing case is always lower than the thrust required using original trim configuration, and the lowest thrust is allowed when twist morphing is used to trim the UAS-S45. Trimming using twist morphing

instead of using elevators would save up to 6.08% of thrust as for the 6<sup>th</sup> flight condition in Fig. 11. Consequently, if the morphing would reduce the thrust force, the global carbon gas emission would also be reduced.

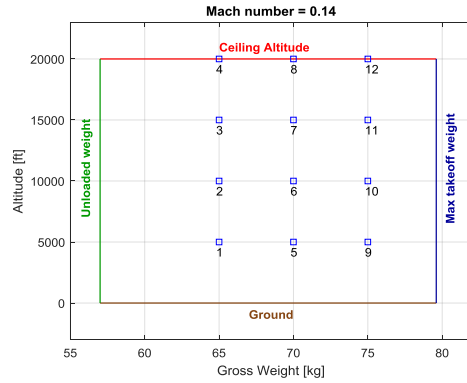


**Figure 10. Flight envelope with flight conditions selected for the study**

In parallel Fig. 12 shows the elevators deflection angle and the morphing angles of twist, dihedral and sweep that were required to trim the UAS-S45 for each flight conditions. On the left hand side of Fig. 12, all the cases were considerate while on the right hand side of the Fig. 12, only elevators and twist angles were considerate because their values are smaller than dihedral and sweep values of angles.

On Fig. 12.a, It can be seen that the sweep angle needs to move from -60 to 95 degrees which is not feasible (the sweep angle could not be set over 80 degrees) consequently, because of the fact that the thrust shown in Fig. 11 was computed according to extrapolated aerodynamic data for flight conditions 8 and 12, these results could not be considered. More generally, if the UAS-S45 could not use the sweep morphing on the whole flight envelope, it could not be considered at all.

Concerning dihedral and twist morphing they seem to be feasible. The dihedral angle needs to move from -18 deg to +84 deg which corresponds to the aerodynamic table computed before. Similarly, the twist angle needs to move from -0.22 deg to 0.76 degrees to trim the UAS-S45 so that the thrust presented for the twist morphing can also be validated. It is interesting to remark that the twist angle needs to move from 0 to 1 degree which corresponds to the same order of mobility of the elevators deflection angle.

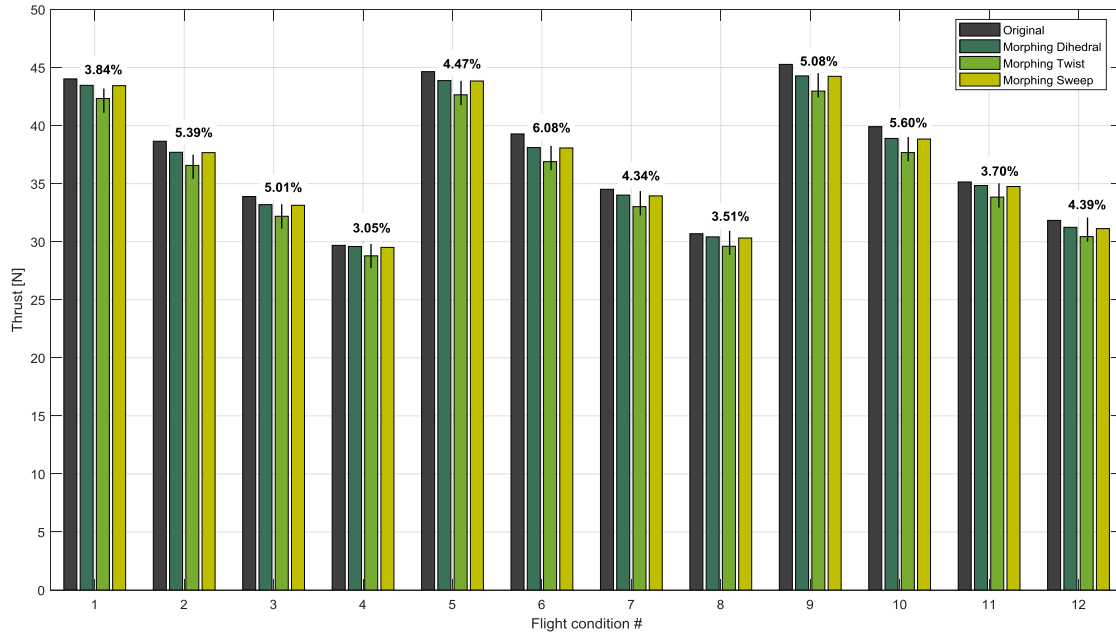


**Figure 11. Thrust required to perform flight conditions using original and morphed aircraft configurations**

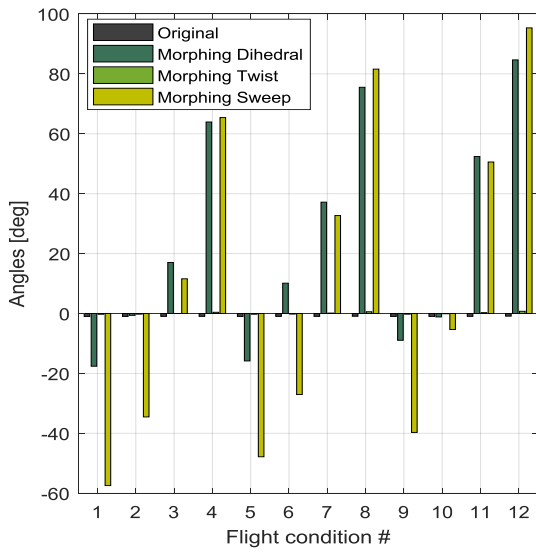


Fig. 12 a)

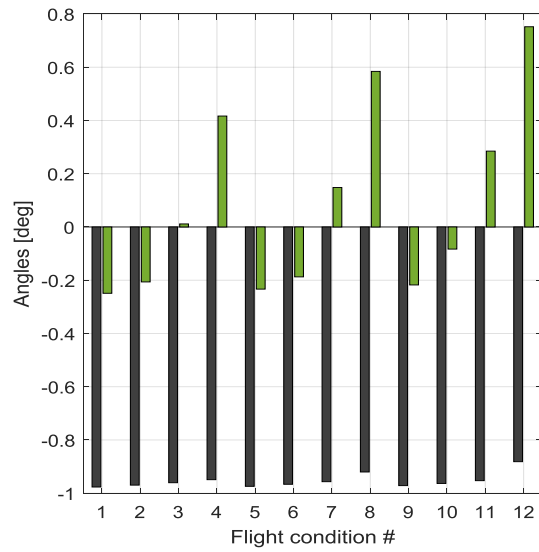


Fig. 12 b)

**Figure 12. Angles of morphing configuration**

## Conclusion

This study has shown that elevators can be replaced by a morphing system to trim an aircraft. Moreover, these morphed configurations allow saving a non-neglected quantity of fuel due to the thrust reduction. It has been shown that the morphing according to the sweep angle of the second part of the horizontal tail was not feasible because of the fact that the aircraft would not have the good aerodynamic characteristics to be trimmed. Dihedral and twist morphing have shown that up to 5% of the thrust can be saved using a twist angle from -0.22 to 0.76 degree or using a dihedral angle moving from -18 to 84 degrees.

From a mechanical point of view, it is sure that the mechanism that could be able to move the twist angle of the horizontal tail of the UAS-S45 will consist in adding some weight on the horizontal tail of the UAS-S45 and consequently it can lose the performance obtained. Meanwhile, on a biggest aircraft, this kind of morphing can be very efficient because the weight that would be added by the morphing system will be practically the same as the weight of the system that would originally trim an aircraft using a stabilizer motion.

## Reference:

- [1] ICAO, "Aviation's Contribution to Climate Change," *ICAO Environmental Report*, 2010.
- [2] A. Hamy, A. Murrieta-Mendoza, and R. Botez, "Flight Trajectory Optimization to Reduce Fuel Burn and Polluting Emissions using a Performance Database and Ant Colony Optimization Algorithm," in *AEGATS '16 Advanced Aircraft Efficiency in a Global Air Transport System*, Paris, France, 2016.
- [3] A. Murrieta Mendoza, "Application of Metaheuristic and Deterministic Algorithms for Aircraft Reference Trajectory Optimization," *École de technologie supérieure*, Montreal, Canada, 2017.
- [4] A. Murrieta Mendoza, A. Bunel, and R. M. Botez, "Aircraft Vertical Reference Trajectory Optimization with a RTA Constraint using the ABC Algorithm," in *16th AIAA Aviation Technology, Integration, and Operations Conference*, 2016, p. 4208.
- [5] A. Murrieta-Mendoza, B. Beuze, L. Ternisien, and R. M. Botez, "New Reference Trajectory Optimization Algorithm for a Flight Management System inspired in Beam Search," *Chinese Journal of Aeronautics*, vol. 30, pp. 1459-1472, 2017.
- [6] A. Murrieta-Mendoza and R. M. Botez, "Methodology for Vertical-Navigation Flight-Trajectory Cost Calculation using a Performance Database," *Journal of Aerospace Information Systems*, vol. 12, pp. 519-532, 2015.
- [7] A. Murrieta-Mendoza, J. Gagné, and R. M. Botez, "New Search Space Reduction Algorithm for Vertical Reference Trajectory Optimization," *INCAS Bulletin*, vol. 8, p. 77, 2016.
- [8] A. Murrieta-Mendoza, L. Ternisien, B. Beuze, and R. M. Botez, "Aircraft Vertical Route Optimization by Beam Search and Initial Search Space Reduction," *Journal of Aerospace Information Systems*, vol. 15, pp. 157-171, 2018.

- [9] R. S. Félix Patrón, Y. Berrou, and R. M. Botez, "Climb, Cruise and Descent 3D Trajectory Optimization Algorithm for a Flight Management System," in *Aviation Technology, Integration, and Operations*, 2014.
- [10] R. S. Félix Patrón, A. Kessaci, and R. M. Botez, "Horizontal Flight Trajectories Optimization for Commercial Aircraft through a Flight Management System," *Aeronautical Journal*, vol. 118, 2014.
- [11] P.-A. Bardela, R. M. Botez, and P. Pageaud, "Cessna Citation X Engine Model Experimental Validation.", in *IASTED Modelling, Identification and Control, Innsbruck, Austria*, 2017.
- [12] M. Zaag and R. M. Botez, "Cessna Citation X Engine Model Identification and Validation in the Cruise Regime from Flight Tests based on Neural Networks combined with Extended Great Deluge Algorithm," in *AIAA Modeling and Simulation Technologies Conference*, 2017, p. 1941.
- [13] C. Hamel, R. Botez, and M. Ruby, "Cessna Citation X Airplane Grey-Box Model Identification without Preliminary Data," SAE Technical Paper 0148-7191, 2014.
- [14] J. R. R. A. Martins, "Fuel Burn Reduction Through Wing Morphing," in *Encyclopedia of Aerospace Engineering, Green Aviation*, ed, 2016, pp. 75-79.
- [15] A. D. Finistauri, "Conceptual Design of a Modular Morphing Wing," Bachelor of Engineering, Ryerson University, 2005.
- [16] O. Ş. Gabor, A. Koreanschi, and R. M. Botez, "Numerical Study of UAS-S4 Ehécatl Aerodynamic Performance Improvement Using a Morphing Wing Technology," in *Unmanned Systems Canada Annual Conference, Montreal, Quebec, Canada*, 2014.
- [17] O. Ş. Gabor, "Validation of Morphing Wing Methodologies on an Unmanned Aerial System and a Wind Tunnel Technology Demonstrator," École de Technologie Supérieure, Montreal, Canada, 2015.
- [18] O. Ş. Gabor, A. Koreaschi, R. M. Botez, M. Mamou, and Y. Mebarki, "Analysis of the Aerodynamic Performance of a Morphing Wing-Tip Demonstrator Using a Novel Nonlinear Vortex Lattice Method," in *the AIAA Conference, Washington, United States*, 2016.
- [19] A. Koreanschi, O. Ş. Gabor, T. Ayrault, R. M. Botez, M. Mamou, and Y. Mebarki, "Numerical Optimization and Experimental Testing of a Morphing Wing with Aileron System," in *24th AIAA/AHS Adaptive Structures Conference*, 2016, p. 1083.
- [20] A. Koreanschi, O. Sugar-Gabor, and R. Botez, "Drag Optimisation of a Wing Equipped with a Morphing Upper Surface," *The Aeronautical Journal*, vol. 120, pp. 473-493, 2016.
- [21] M. Segui, R. M. Botez, "Cessna Citation X Performances Improvement by an Adaptive Winglet during the Cruise Flight," presented at the *World Academy of Science, Engineering and Technology* conference, *Boston, United States*, 2018.
- [22] M. Segui, R. M. Botez, "Cessna Citation X Climb and Cruise Performance Improvement Using Adaptive Winglet," in *the Advanced Aircraft Efficiency in a Global Air Transport System, Toulouse, France*, 2018.
- [23] A. Koreanschi, O. Ş. Gabor, and R. M. Botez, "Drag Optimisation of a Wing Equipped with a Morphing Upper Surface," *The Aeronautical Journal*, vol. 120, pp. 473-493, 2016.

- [24] O. Ş. Gabor, A. Koreanschi, R. M. Botez, M. Mamou, and Y. Mebarki, "Numerical Simulation and Wind Tunnel Tests Investigation and Validation of a Morphing Wing-Tip Demonstrator Aerodynamic Performance," *Aerospace Science and Technology*, vol. 53, pp. 136-153, 2016.
- [25] M. Segui, M. Mantilla, G. Ghazi, and R. M. Botez, "New Economical Cruise Methodology for the Cessna Citation X Business Jet by an Original Morphing Horizontal Tail Application," in *AIAA Modeling and Simulation Technologies Conference*, 2018, p. 3895.
- [26] M. Segui, "Mesure de l'impact de la technologie d'aile déformable sur les performances en croisière de l'avion d'affaire Cessna Citation X," Master, Aerospace, École de Technologie Supérieure, Montreal, 2018.
- [27] NASA, "Vortex-Lattice Utilization," NASA Langley Research Center, Hampton, Virginia 1976.
- [28] R. A. McDonald, "Interactive Reconstruction of 3D Models in the OpenVSP Parametric Geometry Tool," in *53rd AIAA Aerospace Sciences Meeting, American Institute of Aeronautics and Astronautics, Kissimmee, FL*, 2015, pp. 1-10.
- [29] J. R. Gloudemans and R. A. McDonald, "User Defined Components in the OpenVSP Parametric Geometry Tool," in *15th AIAA Aviation Technology, Integration, and Operations Conference, American Institute of Aeronautics and Astronautics, Dallas, TX*, 2015, pp. 1-7.
- [30] M. Segui, R. M. Botez, "Aerodynamic Coefficients Prediction from Minimum Computation Combinations Using OpenVSP Software," in *the World Academy of Science, Engineering and Technology conference, Innsbruck, Austria*, 2018.
- [31] F. P. Bertolotti, T. Herbert, and P. Spalart, "Linear and nonlinear stability of the Blasius boundary layer," *Journal of fluid mechanics*, vol. 242, pp. 441-474, 1992.